Farnesyltransferase inhibitors reverse altered growth and distribution of actin filaments in *Tsc*-deficient cells via inhibition of both rapamycin-sensitive and -insensitive pathways

Chia-Ling Gau, Juran Kato-Stankiewicz, Chen Jiang, Susie Miyamoto, Lea Guo, and Fuyuhiko Tamanoi

Department of Microbiology, Immunology, and Molecular Genetics, Jonsson Comprehensive Cancer Center, Molecular Biology Institute, University of California at Los Angeles, Los Angeles, California

Abstract

Farnesyltransferase inhibitors (FTI) have been developed as anticancer drugs and are currently being evaluated in clinical trials. In this study, we have examined the effects of FTIs on *Tsc*-null cells to gain insight into their effects on farnesylated Rheb GTPase. This protein is involved in the activation of mTOR/S6K signaling and is down-regulated by the Tsc1/Tsc2 complex. Both *Tsc1*$^{-/-}$ and *Tsc2*$^{-/-}$ mouse embryonic fibroblasts exhibit constitutive activation of S6K and grow in the absence of serum. Two different FTI compounds, the clinical compound BMS-214662 and the newly described BMS-225975, inhibit the constitutive activation of mTOR/S6K signaling and block serum-free growth of the *Tsc*-null mouse embryonic fibroblasts. We have also found that *Tsc*-null mouse embryonic fibroblasts grow under anchorage-independent conditions and that both FTI compounds inhibit this soft agar growth. These FTI effects are similar to those observed with rapamycin. Another interesting phenotype of *Tsc*-null mouse embryonic fibroblasts is that they are round and contain actin filaments predominantly at the cell periphery. The addition of FTIs, but not rapamycin, led to the reappearance of intracellular actin filaments and reduction of peripheral actin filaments. The ability of FTI to rearrange actin filaments seems to be largely mediated by the inhibition of Rheb protein, as induction of intracellular actin filaments by FTI was much less efficient in *Tsc2*-null cells expressing Rheb (M184L), a geranylgeranylated mutant Rheb that can bypass farnesylation. These results reveal that FTIs inhibit Rheb, causing two different effects in *Tsc*-deficient cells, one on growth and the other on actin filament distribution. [Mol Cancer Ther 2005;4(6):918–26]

Received 12/28/04; revised 3/3/05; accepted 3/28/05.

Grant support: Supported by NIH grants CA41996 and CA32737.

The costs of publication of this article were defrayed in part by the payment of page charges. This article must therefore be hereby marked advertisement in accordance with 18 U.S.C. Section 1734 solely to indicate this fact.

Note: C-L. Gau and J. Kato-Stankiewicz contributed equally to this work.

Requests for reprints: Fuyuhiko Tamanoi, Department of Microbiology, Immunology, and Molecular Genetics, Jonsson Comprehensive Cancer Center, Molecular Biology Institute, University of California at Los Angeles, 1602 Molecular Sciences Building, Los Angeles, CA 90095. Phone: 310-206-7318; Fax: 310-206-5231. E-mail: fuyut@microbio.ucla.edu

Introduction

Farnesyltransferase inhibitors (FTI) have been developed as anticancer drugs and are currently being evaluated in phase II and phase III clinical trials (1–4). Clinical activities have been observed with hematopoietic malignancies and breast cancer (1–4). One of the recent advances in the development of FTIs is the generation of a novel, highly specific FTI compound BMS-225975 (5). This compound is a derivative of a clinical compound BMS-214662 (6, 7), a tetrahydrobenzodiazepine FTI identified through a screen for a thiol surrogate which could function as a zinc ligand. Replacing the hydrogen on the imidazole of BMS-214662 with a methyl group on the tau nitrogen generated BMS-225975 (5). BMS-225975 exhibits slightly increased potency for farnesylation inhibition. At the same time, BMS-225975 is devoid of the apoptosis induction activity observed with BMS-214662 on some cancer cell lines. With the use of both these compounds, cellular effects due to the inhibition of farnesylation can be more clearly defined.

Although FTIs were initially developed as an inhibitor of Ras proteins, recent studies suggest that there are other target proteins. No correlations between FTI sensitivity and *ras* mutation status have been established (8, 9). Furthermore, K-Ras4B has been shown to be resistant to FTIs, as this protein undergoes geranylgeranylation when farnesylation is inhibited (10, 11). Proposed FTI targets include RhoB, CENP-E,F and Rheb (1, 12). Among these proteins, Rheb is of particular interest. We, as well as others, have recently established that Rheb activates S6K and this activation is inhibited by rapamycin, suggesting that the signaling is mediated through mTOR (13–16). Expression of dominant-negative Rheb mutants blocked nutrient- or serum-induced activation of S6K (17). Rheb also plays important roles in tuberous sclerosis, an autosomal dominant genetic disorder that afflicts 1 in 6,000 to 10,000 individuals (18). The disorder is associated with the appearance of benign tumors called hamartomas at different parts of the body including brain, kidney, lung, and skin (18). Neurologic symptoms include mental retardation, seizure, and autism. A lung disease called lymphagioleiomyomatosis is also associated with tuberous

sclerosis in women (19). Mutations in *TSC1* or *TSC2* genes are responsible for tuberous sclerosis (18). The *TSC1* and *TSC2* gene products form a complex that functions as a GTPase activating protein for Rheb (13–16).

Rheb protein is farnesylated, and our studies in yeast have established that this posttranslational modification is required for the function of Rheb (20). Clark et al. (21) showed that farnesylation facilitates membrane association of mammalian Rheb. Tee et al. (22) reported that a farnesylation defective mutant of Rheb is less efficient in activating S6K, and Castro et al. (23) and Uhlmann et al. (24) showed that FTI inhibits Rheb activation of S6K. On the other hand, Li et al. (25) recently reported that farnesylation is not essential for the function of Rheb to activate S6K. Thus, the significance of farnesylation for the function of mammalian Rheb needs to be further investigated. To gain insight into the effect of FTI on Rheb, we focused on *Tsc*-deficient cells derived from *Tsc* knock-out mice. Homozygous *Tsc* knock-out mice die during embryogenesis due to defects in liver development, whereas heterozygous *Tsc1* or *Tsc2* knock-out mice commonly develop tumors including renal cystadenomas and liver hemangiomas (26, 27). Activation of Rheb has been detected in $Tsc2^{-/-}$ mouse embryonic fibroblasts (28). These mouse embryonic fibroblast cells exhibit constitutive activation of S6K and altered growth properties that include serum-independent growth and loss of contact inhibition (29–31).

In this paper, we show that both FTI compounds inhibit altered growth and signaling properties of $Tsc^{-/-}$ mouse embryonic fibroblasts. We also show that *Tsc*-null mouse embryonic fibroblasts are able to grow in anchorage-independent conditions that can be inhibited by FTIs. We found that the $Tsc2^{-/-}$ mouse embryonic fibroblasts exhibit altered morphology, and actin filaments are predominantly localized in the periphery of cells. FTIs were capable of reversing this phenotype leading to the appearance of intracellular actin filaments and reduction of peripheral actin filaments. Interestingly, rapamycin was incapable of affecting the actin cytoskeleton. By using a mutant Rheb that can bypass farnesylation, we obtained evidence that the effect of FTI on the actin cytoskeleton is mediated by its effect on Rheb. The significance of these observations on the dual role of Rheb on growth and morphology is discussed.

Materials and Methods

Cell Lines and Cell Culture

$Tsc2^{-/-}$ $p53^{-/-}$, $Tsc2^{+/+}$ $p53^{-/-}$, $Tsc1^{-/-}$, and $Tsc1^{+/+}$ mouse embryonic fibroblasts were maintained in DMEM supplemented with 10% (v/v) fetal bovine serum, nonessential amino acids, and penicillin/streptomycin (Life Technologies, Gaithersburg, MD). Human embryonic kidney-293 and COS-7 cells were maintained in DMEM supplemented with 10% (v/v) fetal bovine serum. Human embryonic kidney-293 cells were transiently transfected using the calcium phosphate method. COS-7 and *Tsc2* mouse embryonic fibroblasts were transiently transfected using Polyfect according to the manufacturer (Qiagen, Chatsworth, CA). *Tsc* mouse embryonic fibroblasts were kindly provided by Drs. David Kwiatkowski (Brigham and Women's Hospital) and David Gutmann (Washington University). $Tsc1^{-/-}$ mouse embryonic fibroblasts are spontaneously immortalized, whereas $Tsc2^{-/-}$ mouse embryonic fibroblasts are immortalized by the introduction of *p53* deficiency (26, 31).

Construction of Plasmids

Hemagglutinin-tagged wild-type and mutant Rheb (Rheb1) were subcloned into pCDNA3myc to generate myc-hemagglutinin-tagged Rheb. pCDNA3myc was generated by cloning a linker containing a single myc epitope with the Kozak sequence into the *Hin*dIII/*Nhe*I restriction sites of pCDNA3HA to replace the hemagglutinin epitopes with a myc epitope. pCDNA3HA was generated by cloning triple hemagglutinin tags followed by an *Nhe*I restriction site into the *Hin*dIII/*Eco*RI restriction sites of pCDNA3 (Invitrogen, San Diego, CA). Rheb (C181S) farnesylation-defective mutant and Rheb (M184L) geranylgeranylated mutant were generated by two-step PCR mutagenesis using pCMV5-hemagglutinin-Rheb (WT) as a template (17). Both strands were sequenced to confirm the correct sequence. Mutant hemagglutinin-tagged Rheb cDNAs were subcloned into pCDNA3-myc to generate pCDNA3-mycHARheb (C181S) and pCDNA3-mycHA-Rheb (M184L). pCMV5-Flag-$p70^{S6K}$ was described previously (17).

Cell Viability and Cell Cycle Analysis

Cells (5×10^3) were plated in 96-well plates. For serum starvation experiments, $Tsc2^{-/-}$ and control mouse embryonic fibroblasts were serum-starved in DMEM supplemented with nonessential amino acids (Life Technologies) for 1 to 3 days. $Tsc1^{-/-}$ and control mouse embryonic fibroblasts were starved in DMEM supplemented with 0.1% (v/v) fetal bovine serum, and nonessential amino acids for 1 to 3 days. For drug treatment, $Tsc^{-/-}$ and control mouse embryonic fibroblasts were treated with the appropriate drug in either serum-starved medium (as indicated above) or normal medium for 1 to 3 days. For each time point, 20 μL 2.5 mg/mL 3-(4,5-dimethylthiazol-2-yl)-2,5-diphenyl-tetrazolium bromide (MTT; Sigma, St. Louis, MO) was added to cells in 100 μL of medium and incubated for 2 to 3 hours at 37°C. Cells were lysed in 100 μL of MTT lysis buffer [20% (w/v) SDS, 0.5% (v/v) 80% (v/v) acetic acid, 0.4% (v/v) 1 N HCl, 50% (v/v) *N*,*N*-dimethylformamide] and the absorbance at 570 nm was determined using a Revelation plate reader. The background absorbance at 630 nm was subtracted. Relative cell viability was calculated as a fold-increase from the reading at day 0. Cell cycle profile was analyzed as described previously (32) with the following modifications. Cells ($2–3 \times 10^5$) were plated in 60 mm plates. Rapamycin was obtained from Calbiochem (La Jolla, CA). BMS-225975 and BMS-2214662 were kindly provided by Dr. Veeraswamy Manne (Bristol-Myers Squibb). Other chemicals were obtained from Sigma.

Anchorage-Independent Growth

Soft agar assays were done as described (32) with the following modifications. Mouse embryonic fibroblasts were seeded at densities of 3×10^3 to 10^4 cells per well in a 24-well plate. Images of colonies in soft agar were analyzed at 100× magnification.

Immunoblot Analysis

For serum starvation experiments, 24 hours after seeding, cells were incubated for 24 hours in DMEM supplemented with nonessential amino acids. For drug treatments, cells were treated with the appropriate drug for 48 hours in either serum-free or normal growing medium. Total cell lysates were prepared as described previously (17). Anti-phospho p70 S6K (T389) antibody, anti-phospho S6 (S235/236) antibody, and anti-S6 antibody were obtained from Cell Signaling (Beverly, CA). Anti-p70 S6K antibody was obtained from Santa Cruz (Santa Cruz, CA) and anti-HDJ2 antibody was obtained from NeoMarkers (Fremont, CA) and anti-myc 9B11 was obtained from Cell Signaling.

Immunofluorescence

Tsc2$^{-/-}$ mouse embryonic fibroblasts were treated with various inhibitors as indicated. Cells were stained with anti-myc 9E10 (BAbCO, Richmond, CA) and FITC anti-mouse IgG (Sigma) antibodies or TRITC-phalloidin (Sigma) as described previously (32). Images were analyzed using a Nikon Eclipse TE300 Diaphot microscope with Epifluorescence attachment and a CCD camera system (Photometrics, CoolSNAPfx) supported by the MetaMorph software.

Results

Altered Signaling and Growth Properties of *Tsc*$^{-/-}$ Mouse Embryonic Fibroblasts

Tsc$^{-/-}$ mouse embryonic fibroblasts exhibit a striking change in signaling and growth properties compared with control *Tsc*$^{+/+}$ mouse embryonic fibroblasts. One of the major alterations concerns constitutive activation of mTOR/S6K signaling. The Tsc1/Tsc2 complex functions as a GTPase activating protein for Rheb (13–16), and activation of Rheb is reported in the *Tsc2*$^{-/-}$ mouse embryonic fibroblasts as detected by the increased ratio of GTP/GDP bound to Rheb (28). Figure 1A shows constitutive activation of S6K in *Tsc*$^{-/-}$ mouse embryonic fibroblasts as detected by the use of an antibody specific to phospho-S6K (T389). With the control *Tsc1*$^{+/+}$ mouse embryonic fibroblasts, phosphorylation of S6K was decreased upon serum starvation and induced at a high level only after the addition of serum (Fig. 1A, *left*). In contrast, phosphorylation of S6K was constitutively up-regulated in *Tsc1*$^{-/-}$ mouse embryonic fibroblasts even in the absence of serum. Similar constitutive activation of S6K was observed in *Tsc2*$^{-/-}$ mouse embryonic fibroblasts (Fig. 1A, *right*). In addition, S6, a downstream substrate of S6K, was also constitutively activated in *Tsc*$^{-/-}$ mouse embryonic fibroblasts (data not shown). Our results agree with those of previous studies (26, 29, 31).

In addition, *Tsc*$^{-/-}$ mouse embryonic fibroblasts grow in the absence of serum. *Tsc2*$^{-/-}$ cells continue to grow after serum withdrawal, whereas *Tsc2*$^{+/+}$ mouse embryonic fibroblasts stop growing (Fig. 1B, *right*). Similar serum-independency was observed with *Tsc1*$^{-/-}$ mouse embryonic fibroblasts (Fig. 1B, *left*). Serum-independent growth was more pronounced with *Tsc2*$^{-/-}$ mouse embryonic fibroblasts, which may reflect the lack of *p53* in this cell line (31). The serum-independent growth of *Tsc2*$^{-/-}$ mouse embryonic fibroblasts was further investigated by examining their cell cycle profiles. As shown in Fig. 1C, the cell cycle profile of *Tsc2*$^{-/-}$ mouse embryonic fibroblasts was not affected upon serum withdrawal, whereas it led to a significant accumulation of G_0/G_1 phase cells in *Tsc2*$^{+/+}$ cells. Treatment of *Tsc2*$^{-/-}$ mouse embryonic fibroblasts with rapamycin resulted in increase of G_0/G_1 phase cells, suggesting that the serum-independent growth phenotype is mediated through the mTOR pathway and that the cell cycle machinery involved in G_1-S transition is intact. Similar results were obtained when we examined the cell cycle profiles of these cells at high confluency. *Tsc2*$^{-/-}$ mouse embryonic fibroblasts failed to arrest at G_0/G_1 phase, whereas significant accumulation of G_0/G_1 phase cells was observed with *Tsc2*$^{+/+}$ mouse embryonic fibroblasts (Fig. 1D). Although *Tsc2*$^{-/-}$ mouse embryonic fibroblasts showed higher saturation densities than *Tsc2*$^{+/+}$ mouse embryonic fibroblasts, they did not form foci when we did a focus formation assay (data not shown).

FTIs Inhibit Altered mTOR/S6K Signaling and Growth Properties of *Tsc*-Null Mouse Embryonic Fibroblasts

To examine the effects of FTIs on the altered signaling and growth properties of *Tsc*-null mouse embryonic fibroblasts, we used two different FTI compounds, BMS-214662 and BMS-225975. These compounds inhibit the protein farnesyltransferase reaction *in vitro* with IC_{50} value of ~1 nmol/L. *In vivo*, BMS-214662 and BMS-225975 induce reversion of H-*ras* transformed Rat1 cells with IC_{50} values of 0.1 and 0.02 μmol/L, respectively (5). Figure 2A shows that BMS-214662 and BMS-225975 inhibit farnesylation of ectopically expressed Rheb and cause a mobility shift to a slower migrating unmodified form with concentrations as little as 0.25 μmol/L in human embryonic kidney-293 cells. BMS-225975 was slightly more potent than BMS-214662, in agreement with its increased ability to inhibit farnesylation. The farnesylation defective mutant of Rheb, Rheb (C181S), was expressed as a control unmodified form. Figure 2B shows the effect of FTIs on S6K activation induced by the expression of Rheb. Under starved conditions, overexpressed S6K is not phosphorylated in COS-7 cells. However, coexpression with Rheb significantly induced phosphorylation of S6K. This Rheb-induced activation of S6K was inhibited by the treatment of cells with 1 μmol/L BMS-225975. In addition, Rheb (C181S), did not activate S6K (Fig. 2B).

Both FTI compounds were capable of inhibiting the constitutive activation of S6K and S6 in *Tsc*$^{-/-}$ mouse embryonic fibroblasts. *Tsc*$^{-/-}$ mouse embryonic fibroblasts were treated with BMS-225975 or rapamycin in serum-free medium. Figure 2C shows that phosphorylation of S6K in the *Tsc1*$^{-/-}$ mouse embryonic fibroblasts was inhibited by the incubation with BMS-225975 in a dose-dependent manner.

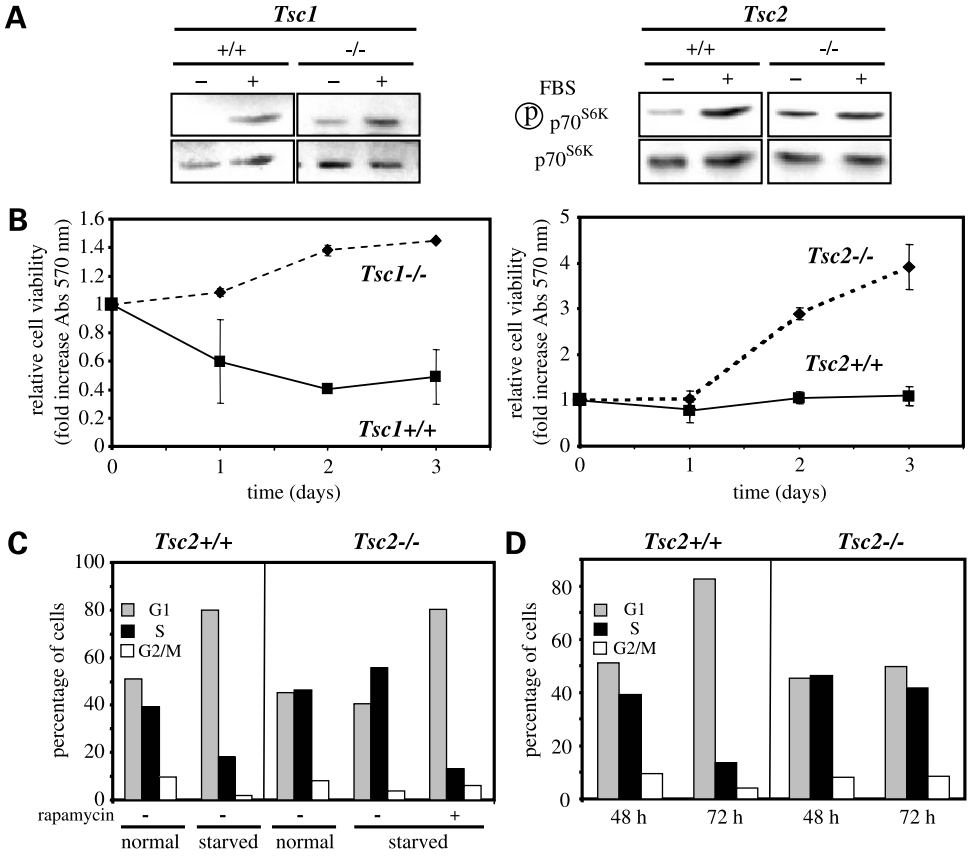

Figure 1. **A,** *Tsc*-null mouse embryonic fibroblasts have a higher level of S6K phosphorylation than control mouse embryonic fibroblasts in serum-starved conditions. Cells were starved for 24 h (–). Cells were starved and then stimulated for 15 min with 20% fetal bovine serum (+). Phosphorylated and total levels of S6K were examined as described in Materials and Methods. Results are representative of three independent experiments. **B,** growth of *Tsc1*$^{-/-}$ and control mouse embryonic fibroblasts in serum-free medium (*left*); growth of T*sc2*$^{-/-}$ and control mouse embryonic fibroblasts in serum-free medium (*right*). Twenty-four hours after seeding, cells were changed to medium without serum. Cell viability was assayed using an MTT assay. *Points,* means; *bars,* SD. **C,** *Tsc2*$^{-/-}$ mouse embryonic fibroblasts do not arrest in G_0/G_1 during serum starvation. *Tsc2* mouse embryonic fibroblasts were collected at 60% confluency, whereas they were exponentially growing in normal medium or after serum starvation for 24 h. Cell cycle profile was then analyzed as described in Materials and Methods. Results are representative of three independent experiments. **D,** cell cycle profile of *Tsc2*$^{-/-}$ mouse embryonic fibroblasts were analyzed in exponentially growing conditions (48 h, 60% confluency) or in contact inhibited conditions (72 h, 100% confluent). Results are representative of three independent experiments.

Constitutive activation of S6 was also inhibited by the treatment with BMS-225975 in the *Tsc2*$^{-/-}$ mouse embryonic fibroblasts. The inhibition of farnesylation was assessed by the shift in mobility of HDJ-2, a farnesylated chaperone protein commonly used as a marker for the inhibition of farnesylation (33).

The effects of FTIs on the serum-independent growth of *Tsc*$^{-/-}$ mouse embryonic fibroblasts were examined (Fig. 2D). Both BMS-225975 and BMS-214662 were able to inhibit the serum-free growth of *Tsc2*$^{-/-}$ mouse embryonic fibroblasts. After incubation for 2 to 3 days, FTIs' effects were similar to those observed with rapamycin. The effects of FTIs required prolonged incubation, whereas the rapamycin effect was more immediate, presumably reflecting the fact that FTIs inhibit farnesylation of newly synthesized proteins and cannot inhibit the function of preexisting farnesylated proteins. With *Tsc1*$^{-/-}$ mouse embryonic fibroblast, BMS-225975 showed significant inhibition, whereas the effects of BMS-214662 were weak.

Tsc$^{-/-}$ Mouse Embryonic Fibroblasts Exhibit Anchorage-Independent Growth and This Phenotype Is Inhibited by FTI

Another striking feature of *Tsc*-null cells is their ability to grow under anchorage-independent conditions. We examined growth of *Tsc*$^{-/-}$ mouse embryonic fibroblasts derived from *Tsc* knock-out mice in soft agar and found that the *Tsc*$^{-/-}$ mouse embryonic fibroblasts can grow in soft agar when seeded at high densities. As can be seen in Fig. 3A, both *Tsc1*$^{-/-}$ and *Tsc2*$^{-/-}$ mouse embryonic fibroblasts form multicellular colonies in soft agar particularly when plated at high densities, whereas this growth was not observed with the control wild-type mouse embryonic fibroblasts. Anchorage-independent growth was more pronounced with *Tsc2*$^{-/-}$ mouse embryonic fibroblasts, which may be due to the lack of *p53* in this cell line (31). The ability of *Tsc2*$^{-/-}$ mouse embryonic fibroblasts to grow in an anchorage-independent manner is also supported by our observation that they grow on a plate

coated with polyHEMA (data not shown). The anchorage-independent growth of *Tsc*-null mouse embryonic fibroblasts we observed, however, was not as vigorous as those of other human cancer–derived cell lines or *ras*-transformed fibroblasts. This agrees with the observation that a special condition (a higher concentration of agar compared with conventional conditions used for human cancer derived cell lines) is needed, in this case, to detect anchorage-independent growth of $Tsc2^{-/-}$ fibroblasts derived from Eker rat (34).

Figure 3B shows the effect of FTIs on the anchorage-independent growth of *Tsc*-null mouse embryonic fibroblasts. Treatment of $Tsc1^{-/-}$ mouse embryonic fibroblasts as well as $Tsc2^{-/-}$ mouse embryonic fibroblasts with BMS-214662 or BMS-225975 effectively inhibited the formation of colonies in soft agar. Inhibition of anchorage-independent growth was also observed with rapamycin and LY294002.

Tsc2-Null Mouse Embryonic Fibroblasts Exhibit Altered Morphology and Actin Filament Distribution in a FTI-Sensitive and Rapamycin-Insensitive Manner

The above results show that FTIs are capable of inhibiting serum-free as well as anchorage-independent growth of *Tsc*-null cells and that these effects seem to be due to their effects on the inhibition of S6K. These effects are similar to those elicited by rapamycin, an inhibitor of the mTOR/raptor complex. We have observed additional effects of FTIs that seem to be independent of the mTOR/raptor complex inhibition. Viewed under a phase-contrast microscope, $Tsc2^{-/-}$ mouse embryonic fibroblasts exhibit altered morphology compared with the control mouse embryonic fibroblasts. $Tsc2^{-/-}$ mouse embryonic fibroblasts seem rounded, whereas the control mouse embryonic fibroblasts are stretched out with the typical fibroblastic extensions. Phalloidin staining revealed differences in the distribution of actin filaments in the $Tsc2^{-/-}$ and the control mouse embryonic fibroblasts. Although actin filaments are dispersed intracellularly in the control $Tsc2^{+/+}$ mouse embryonic fibroblasts (Fig. 4, *top left*), actin filaments are assembled mainly at the cell periphery, reminiscent of lamellipodia, in $Tsc2^{-/-}$ mouse embryonic fibroblasts (Fig. 4, *top right*).

Effects of FTI on the morphology of these mouse embryonic fibroblasts have been examined. With $Tsc2^{+/+}$ mouse embryonic fibroblasts, no major changes in actin filaments were observed upon treatment with FTIs (Fig. 4, *left*). In contrast, treatment of the $Tsc2^{-/-}$ mouse embryonic fibroblasts with FTIs resulted in the reduction of peripheral actin and redistribution of intracellular actin filaments (Fig. 4, *right*). These intracellular actin filaments are well aligned, similar to what is seen in the $Tsc2^{+/+}$

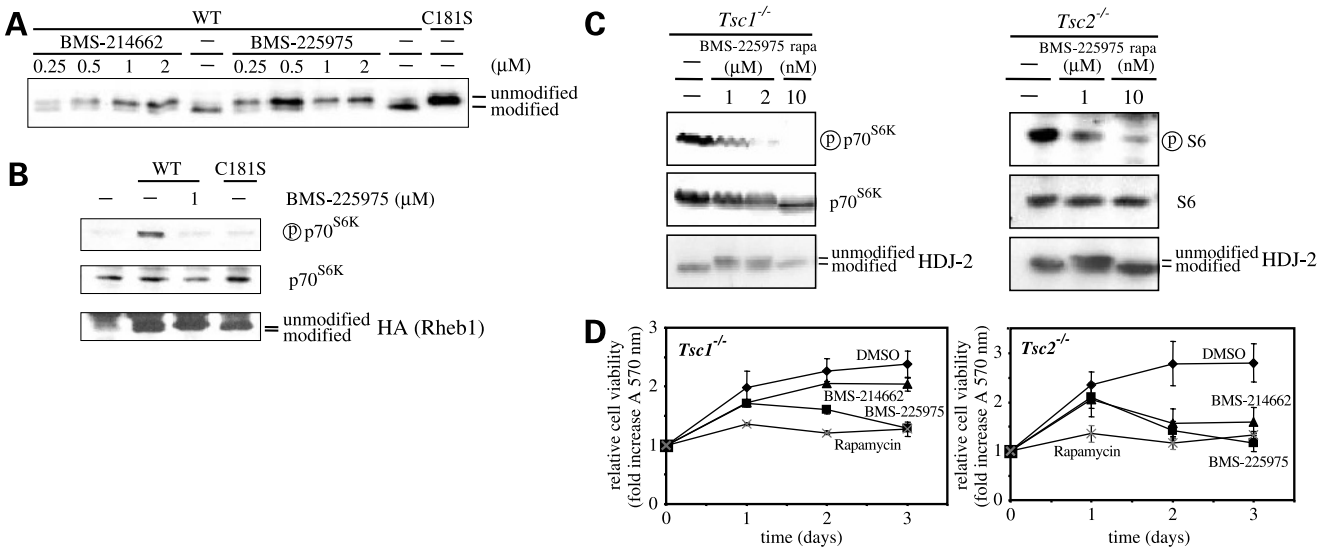

Figure 2. **A,** FTIs inhibit the farnesylation of Rheb. pCDNA3mycHA-Rheb (WT and C181S) were transiently expressed in human embryonic kidney-293 cells. Cells were treated for 24 h with the indicated concentration of FTI starting 16 h after transfection. Rheb expression was detected by immunoblotting with anti-myc 9B11 antibody. Results shown are representative of three independent experiments. **B,** farnesylation is required for the activation of S6K by Rheb. pCMV5-hemagglutinin-Rheb (WT and C181S) and pCMV5-Flag-$p70^{S6K}$ were transiently coexpressed in COS-7 cells. Cells were pretreated with the indicated concentration of BMS-225975 for 24 h, and then starved in PBS for 30 min. Phosphorylated and total levels of S6K were examined as described in Materials and Methods. Rheb expression was confirmed by the use of anti-hemagglutinin antibody. **C,** $Tsc1^{-/-}$ mouse embryonic fibroblasts (*left*) and $Tsc2^{-/-}$ mouse embryonic fibroblasts (*right*) were treated with 1 or 2 μmol/L BMS-225975 or 10 nmol/L rapamycin in serum-free medium for 48 h. Phosphorylated and total levels of S6K or S6 were examined as described in Materials and Methods. Inhibition of farnesylation was confirmed by the mobility shift of HDJ-2 protein. Results are representative of three independent experiments. **D,** $Tsc^{-/-}$ mouse embryonic fibroblasts were plated in 96-well plates, and after 24 h, medium was changed to serum-free medium and the indicated drug (day 0). Cells were treated with 1 μmol/L BMS-214662 or BMS-225975, or 10 nmol/L rapamycin. Cell viability was then assayed by MTT assay at the indicated times. $Tsc1^{-/-}$ mouse embryonic fibroblasts (*left*) and $Tsc2^{-/-}$ $Tsc2^{-/-}$ mouse embryonic fibroblasts (*right*). *Points,* means; *bars,* SD.

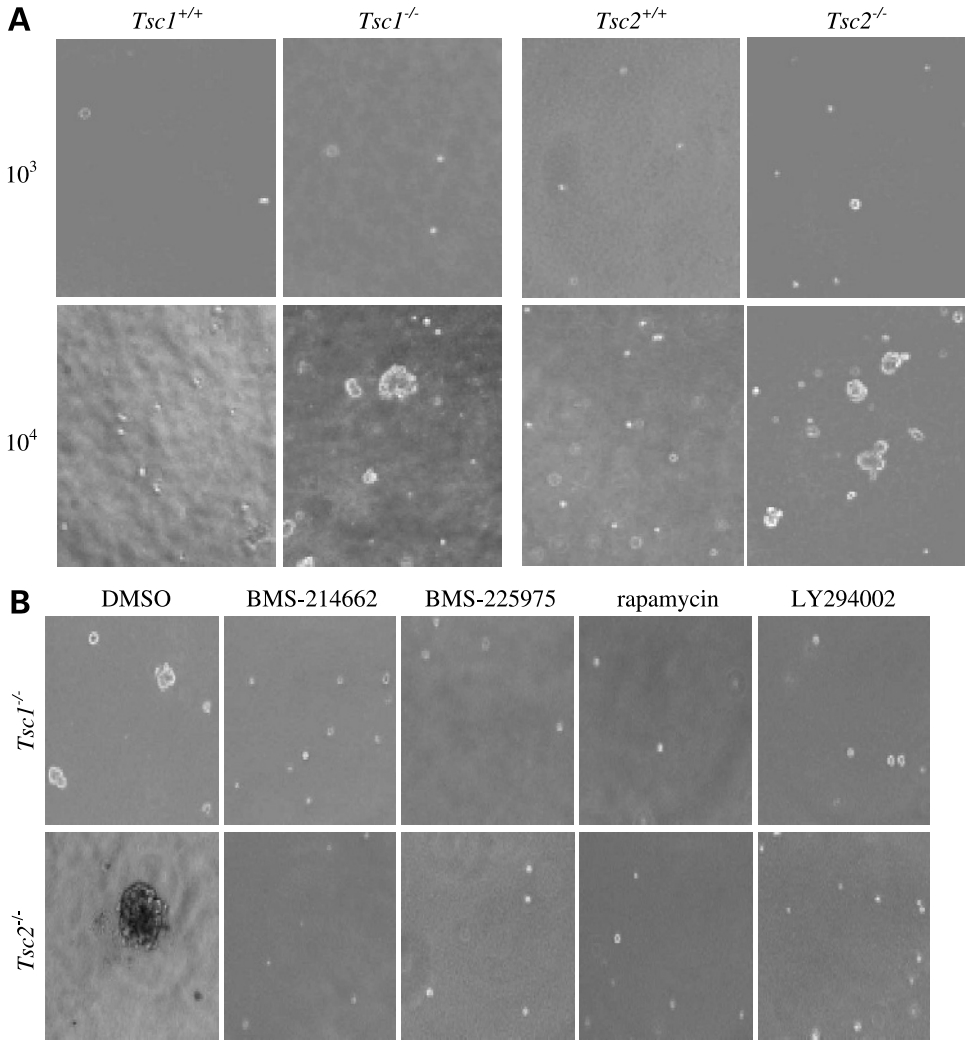

Figure 3. FTIs can inhibit the anchorage-independent growth of *Tsc*$^{-/-}$ mouse embryonic fibroblasts. **A**, *Tsc*-null mouse embryonic fibroblasts are able to grow in soft agar. Mouse embryonic fibroblasts were cultured in soft agar for 2 wks at different densities, i.e., 3×10^3 cells per well (*top*) or 3×10^4 cells per well (*bottom*). Results are representative of three independent experiments. **B**, *Tsc1*$^{-/-}$ mouse embryonic fibroblasts (*top*) and *Tsc2*$^{-/-}$ mouse embryonic fibroblasts (*bottom*) were cultured for 2 wks in soft-agar in the presence of various inhibitors as indicated (0.25 μmol/L FTIs, 2.5 nmol/L rapamycin or 33 μmol/L LY249002). Results are representative of three independent experiments.

mouse embryonic fibroblasts. A more potent FTI compound BMS-225975 induced changes in cell morphology. In contrast to the results with FTIs, treatment with rapamycin did not affect the distribution of actin cytoskeleton in the *Tsc2*$^{-/-}$ and *Tsc2*$^{+/+}$ mouse embryonic fibroblasts (Fig. 4, *bottom*).

Effect of FTIs on Actin Cytoskeleton Is Mediated by the Inhibition of Rheb

The above effect of FTIs on actin cytoskeleton is of particular interest, as this is not observed with rapamycin. To examine whether this FTI effect is mediated by the inhibition of Rheb, we expressed a mutant form of Rheb that can bypass the farnesylation requirement. This was accomplished by mutating the COOH-terminal methionine to leucine, thus converting the CaaX motif to the CaaL motif (1, 35). The CaaL motif is recognized by geranylgeranyltransferase type I, and the resulting mutant protein can be modified by geranylgeranylation instead of farnesylation. Thus, expression of the mutant Rheb, Rheb (M184L), is expected to generate cells that are resistant to FTI. *Tsc2*-null mouse embryonic fibroblasts were transiently transfected with the myc-tagged Rheb (M184L) and effects on actin filaments in the cells expressing Rheb (M184L) were examined by costaining with anti-myc antibody and phalloidin (Fig. 5). First, we confirmed that expression of Rheb (M184L) itself did not alter actin distribution in *Tsc2*$^{-/-}$ mouse embryonic fibroblasts (see Fig. 5, DMSO). Expression of Rheb (M184L) also did not cause any evident change in the peripheral actin in *Tsc2*$^{+/+}$ mouse embryonic fibroblasts (data not shown). We next examined if there is a differential response to FTIs with or without expression of mutant Rheb in *Tsc2*$^{-/-}$ mouse embryonic fibroblasts. As shown in Fig. 5, the cells expressing Rheb (M184L) were resistant to the effect of FTIs as both BMS-214662 or BMS-225975 failed to induce intracellular actin and the peripheral accumulation of actin remained unchanged. In contrast, the actin cytoskeleton in cells not expressing Rheb (M184L) was significantly affected by FTI treatment. These results suggest that expression of the mutant Rheb confers resistance to FTIs in *Tsc2*$^{-/-}$ mouse embryonic fibroblasts.

Discussion

FTIs are capable of inhibiting Rheb farnesylation. FTIs inhibit constitutive activation of S6K and S6 in *Tsc*-null mouse embryonic fibroblasts. Serum-independent growth as well as anchorage-independent growth of these cells is inhibited by FTIs. To confirm that the effects of FTIs reflect their inhibition of farnesylation, we used two different FTI compounds. Both compounds elicited similar effects. In addition, we have observed a correlation between the concentrations of FTIs needed to inhibit the altered growth phenotypes of *Tsc*-null mouse embryonic fibroblasts and those needed to inhibit farnesylation of Rheb as well as HDJ-2 proteins. These results, taken together, strongly suggest that FTIs are capable of inhibiting Rheb's function to activate mTOR/S6K. The observation that rapamycin causes effects similar to those seen with FTI further supports this idea.

Our results showing that FTIs have the ability to inhibit altered growth and signaling properties of $Tsc^{-/-}$ mouse embryonic fibroblasts with potency comparable to that observed with rapamycin raises the possibility that FTIs provide an effective reagent to treat benign tumors in tuberous sclerosis. It will be interesting to examine whether FTIs can elicit tumor response similar to that observed with rapamycin in *Tsc*-deficient mice or in the Eker rat. Rapamycin has been shown to reduce proliferation of tumor cells and prolong survival of Eker rats that carry a germ line *Tsc2* mutation (36, 37). Decreased serum vascular endothelial growth factor levels and apoptosis in tumors were detected in $Tsc1^{+/-}$ mice treated with rapamycin (38). The availability of multiple drugs that can influence *Tsc*-deficient phenotypes represents an important advance towards developing effective therapy against tuberous sclerosis. Another implication of our work is that FTIs may be effective in inhibiting transformed phenotypes of human cancer cells with Rheb activation. In prostate cancer, Akt is frequently activated due to the loss of *Pten*, thus, leading to the activation of the Akt/mTOR/S6K signaling (39). Her2 overexpression is seen in a significant percentage of breast cancer (40), which results in the activation of Akt (41). It will be important to examine whether Rheb is activated in human cancer cell lines that have the activation of the phosphoinositide-3-kinase/mTOR signaling pathway, and to investigate the effect of FTIs on theses cell lines.

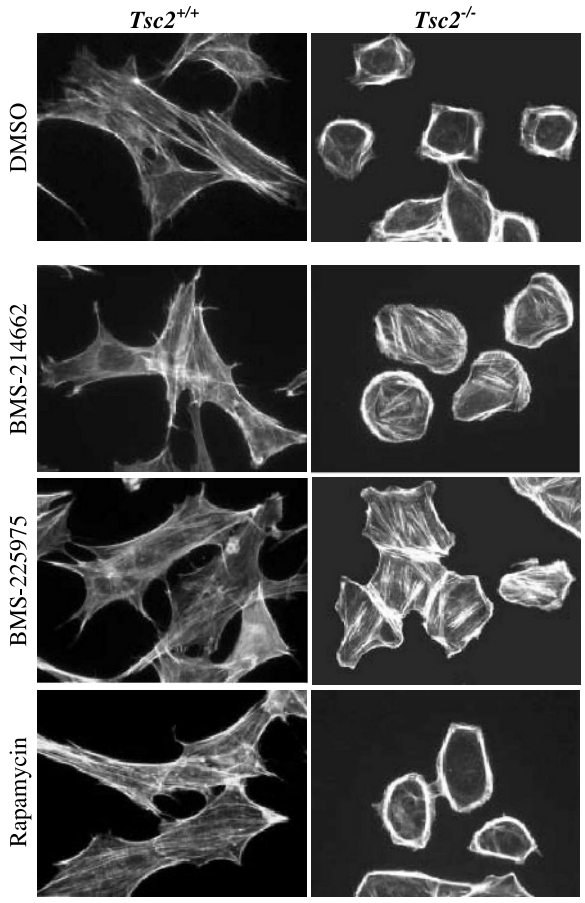

Figure 4. FTIs induced the rearrangement of actin cytoskeleton in $Tsc2^{-/-}$ mouse embryonic fibroblasts. Tsc2 mouse embryonic fibroblasts were treated with DMSO, FTIs (2 μmol/L) or rapamycin (10 nmol/L) for 72 h in normal growth medium. Actin filaments of $Tsc2^{+/+}$ (*left*) and $Tsc2^{-/-}$ (*right*) mouse embryonic fibroblasts were visualized by TRITC-phalloidin as indicated in Materials and Methods. Results are representative of three independent experiments.

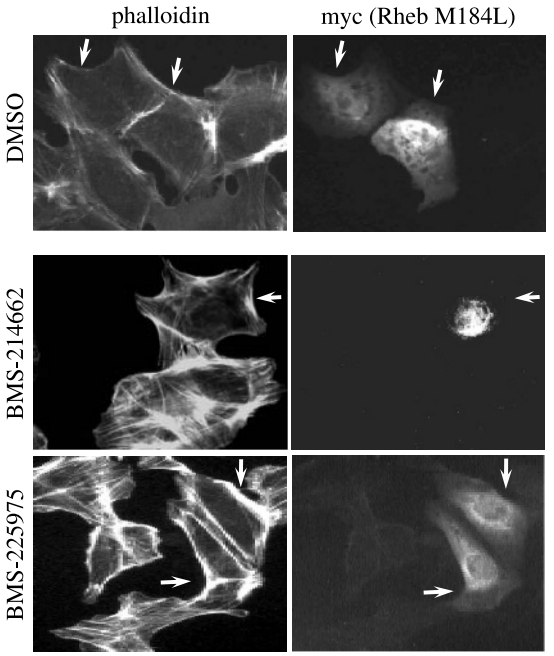

Figure 5. $Tsc2^{-/-}$ mouse embryonic fibroblasts overexpressing myc-tagged Rheb (M184L) are resistant to FTI-induced rearrangement of actin cytoskeleton. Overnight after transfection, cells were treated with or without FTIs (2 μmol/L) and actin filaments were visualized by TRITC-phalloidin as described in Materials and Methods (*left*). Rheb expressing cells detected by anti-myc antibody and FITC anti-mouse antibody are indicated with *arrows* (*right*). Results are representative of three independent experiments.

Our study with FTI uncovered another role of Rheb in *Tsc*-null cells. First, we noticed that $Tsc2^{-/-}$ mouse embryonic fibroblast cells appear as rounded cells, whereas the control $Tsc2^{+/+}$ mouse embryonic fibroblast cells are stretched out. In the $Tsc2^{-/-}$ mouse embryonic fibroblasts, actin filaments were predominantly assembled around the cell periphery giving an appearance resembling lamellipodia and membrane ruffles. In addition, these cells have increased adherence compared with the control cells.[1] The peripheral actin distribution in $Tsc2^{-/-}$ mouse embryonic fibroblasts we observed is different from the distribution of actin filaments in the Eker rat–derived smooth muscle cells recently reported by Goncharova et al. (42). This apparent difference is presumably due to the difference in cell lines used. We further showed that the treatment with FTIs leads to the rearrangement of actin filaments specifically in $Tsc2^{-/-}$ mouse embryonic fibroblasts but not in control mouse embryonic fibroblasts. This FTI effect is mediated by the inhibition of Rheb, as shown by the use of a Rheb mutant that can bypass farnesylation: overexpression of a geranylgeranylated Rheb mutant conferred $Tsc2^{-/-}$ mouse embryonic fibroblasts resistance to the FTI. Thus, Rheb is involved in rearrangement of actin cytoskeleton in $Tsc2^{-/-}$ mouse embryonic fibroblasts. It has been reported that Tsc1 interacts with the ERM proteins and activates Rho (43) and regulates the assembly of intracellular actin filaments (42, 43). Activation of Rho by Tsc2 has also been reported (44). Further work is needed to clarify the contribution of Tsc1/2 and Rheb to the regulation of the actin cytoskeleton.

It is interesting that rapamycin was incapable of affecting the actin cytoskeleton. These results suggest that there are two distinct pathways downstream of Rheb, one signaling to growth and the other affecting the actin cytoskeleton. The pathway affecting growth is rapamycin-sensitive and is likely to involve a rapamycin-sensitive mTOR complex that contains raptor and signals to S6K (45). On the other hand, the pathway affecting actin cytoskeleton is rapamycin-insensitive. What pathway could be responsible for the effect? We initially considered the possibility that FTI suppresses the inhibitory action of Rheb on B-Raf (46, 47), resulting in the activation of the MEK/ROCKII/LIMK/cofilin signaling pathway (48). However, this seems unlikely because MEK inhibitors, PD98059 and U0126, showed no effects on actin filaments in *Tsc2* mouse embryonic fibroblasts.[1] A more likely possibility involves a recently identified second mTOR complex, mTORC2. The mTORC2 contains a novel protein Rictor/mAVO3 and mediates signals to actin cytoskeleton in a rapamycin-insensitive manner (49, 50). Inactivation of mTORC2 components causes decreased Rac activity, which in turn leads to rearrangement of the actin cytoskeleton: decrease in the cortical actin, cell spreading, and adhesion and increase in cytoplasmic actin filaments (49, 50). Our findings of lamellipodia-like peripheral actin distribution and increase in adhesion in $Tsc2^{-/-}$ mouse embryonic fibroblasts suggest that mTORC2 plays an important role in the phenotypes of $Tsc2^{-/-}$ mouse embryonic fibroblasts. With our observation that FTI affects both growth and actin cytoskeleton in $Tsc2^{-/-}$ mouse embryonic fibroblasts through the inhibition of Rheb, it is tempting to speculate that Rheb transmits signals not only to the mTOR/raptor complex but also to the mTORC2. Further experiments using FTIs may provide important insight into how Rheb influences growth and actin cytoskeleton.

[1] J. Kato-Stankiewicz and F. Tamanoi, unpublished observation.

Acknowledgments

We thank Drs. David Gutmann and David Kwiatkowski for valuable advice throughout this work and for providing the $Tsc^{-/-}$ and control mouse embryonic fibroblasts; Drs. Junji Yamauchi and Jun Urano for providing expression vectors; Dr. Veeraswamy Manne, who not only provided the FTI compounds used in this study but also provided valuable comments about this manuscript; and Drs. Angel Tabancay and Nitika Parmer as well as Kathleen Averente, Melissa Comiso, P.J. Aspuria, and Parthive Patel for discussion and critical reading of our manuscript. The flow cytometric analysis was done in the University of California at Los Angeles Flow Cytometry Core Facilities that are supported in part by grants from the NIH (CA16042 and AI28697).

References

1. Tamanoi F, Gau CL, Jiang C, Edamatsu H, Kato-Stankiewicz J. Protein farnesylation in mammalian cells: effects of farnesyltransferase inhibitors on cancer cells. Cell Mol Life Sci 2001;58:1636 – 49.

2. Brunner TB, Hahn SM, Gupta AK, Muschel RJ, McKenna WG, Bernhard EJ. Farnesyltransferase inhibitors: an overview of the results of preclinical and clinical investigations. Cancer Res 2003;63:5656 – 68.

3. O'Regan RM, Khuri FR. Farnesyl transferase inhibitors: the next targeted therapies for breast cancer? Endocr Relat Cancer 2004;11:191 – 205.

4. Doll RJ, Kirschmeier P, Bishop WR. Farnesyltransferase inhibitors as anticancer agents: critical crossroads. Curr Opin Drug Discov Devel 2004;7:478 – 86.

5. Manne V, Lee FY, Bol DK, et al. Apoptotic and cytostatic farnesyltransferase inhibitors have distinct pharmacology and efficacy profiles in tumor models. Cancer Res 2004;64:3974 – 80.

6. Hunt JT, Ding CZ, Batorsky R, et al. Discovery of (*R*)-7-cyano-2,3,4,5-tetrahydro-1-(1H-imidazol-4-ylmethyl)-3-(phenylmethyl)-4-(2-thienylsulfonyl)-1H-1,4-benzodiazepine (BMS-214662), a farnesyltransferase inhibitor with potent preclinical antitumor activity. J Med Chem 2000;43:3587 – 95.

7. Rose WC, Lee FY, Fairchild CR, et al. Preclinical antitumor activity of BMS-214662, a highly apoptotic and novel farnesyltransferase inhibitor. Cancer Res 2001;61:7507 – 17.

8. Sepp-Lorenzino L, Ma Z, Rands E, et al. A peptidomimetic inhibitor of farnesyl:protein transferase blocks the anchorage-dependent and -independent growth of human tumor cell lines. Cancer Res 1995;55:5302 – 9.

9. End DW, Smets G, Todd AV, et al. Characterization of the antitumor effects of the selective farnesyl protein transferase inhibitor R115777 *in vivo* and *in vitro*. Cancer Res 2001;61:131 – 7.

10. Rowell CA, Kowalczyk JJ, Lewis MD, Garcia AM. Direct demonstration of geranylgeranylation and farnesylation of Ki-Ras *in vivo*. J Biol Chem 1997;272:14093 – 7.

11. Whyte DB, Kirschmeier P, Hockenberry TN, et al. K- and N-ras are geranylgeranylated in cells treated with farnesyl protein transferase inhibitors. J Biol Chem 1997;272:14459 – 64.

12. Sebti SM, Der CJ. Opinion: Searching for the elusive targets of farnesyltransferase inhibitors. Nat Rev Cancer 2003;3:945 – 51.

13. Harris TE, Lawrence JC Jr. TOR signaling. Sci STKE 2003;2003:re15.

14. Manning BD, Cantley LC. Rheb fills a GAP between TSC and TOR. Trends Biochem Sci 2003;28:573 – 6.

15. Pan D, Dong J, Zhang Y, Gao X. Tuberous sclerosis complex: from *Drosophila* to human disease. Trends Cell Biol 2004;14:78 – 85.

16. Aspuria PJ, Tamanoi F. The Rheb family of GTP binding proteins. Cell Signal 2004;16:1105 – 12.

17. Tabancay AP Jr, Gau CL, Machado IM, et al. Identification of dominant negative mutants of Rheb GTPase and their use to implicate the involvement of human Rheb in the activation of p70S6K. J Biol Chem 2003;278:39921 – 30.

18. Gomez M, Sampson J, Whittemore V. The tuberous sclerosis complex. Oxford, UK: Oxford University Press; 1999.

19. Carsillo T, Astrinidis A, Henske EP. Mutations in the tuberous sclerosis complex gene TSC2 are a cause of sporadic pulmonary lymphangioleiomyomatosis. Proc Natl Acad Sci U S A 2000;97:6085 – 90.

20. Yang W, Tabancay AP Jr, Urano J, Tamanoi F. Failure to farnesylate Rheb protein contributes to the enrichment of G_0/G_1 phase cells in the *Schizosaccharomyces pombe* farnesyltransferase mutant. Mol Microbiol 2001;41:1339 – 47.

21. Clark GJ, Kinch MS, Rogers-Graham K, Sebti SM, Hamilton AD, Der CJ. The Ras-related protein Rheb is farnesylated and antagonizes Ras signaling and transformation. J Biol Chem 1997;272:10608 – 15.

22. Tee AR, Manning BD, Roux PP, Cantley LC, Blenis J. Tuberous sclerosis complex gene products, Tuberin and Hamartin, control mTOR signaling by acting as a GTPase-activating protein complex toward Rheb. Curr Biol 2003;13:1259 – 68.

23. Castro AF, Rebhun JF, Clark GG, Quilliam LA. Rheb binds TSC2 and promotes S6 kinase activation in a rapamycin- and farnesylation-dependent manner. J Biol Chem 2003;278:32493 – 6.

24. Uhlmann EJ, Li W, Scheidenhelm DK, Gau CL, Tamanoi F, Gutmann DH. Loss of tuberous sclerosis complex 1 (Tsc1) expression results in increased Rheb/S6K pathway signaling important for astrocyte cell size regulation. Glia 2004;47:180 – 8.

25. Li Y, Inoki K, Guan KL. Biochemical and functional characterizations of small GTPase Rheb and TSC2 GAP activity. Mol Cell Biol 2004;24: 7965 – 75.

26. Kwiatkowski DJ, Zhang H, Bandura JL, et al. A mouse model of TSC1 reveals sex-dependent lethality from liver hemangiomas, and up-regulation of p70S6 kinase activity in Tsc1 null cells. Hum Mol Genet 2002;11: 525 – 34.

27. Onda H, Lueck A, Marks PW, Warren HB, Kwiatkowski DJ. Tsc2(+/–) mice develop tumors in multiple sites that express gelsolin and are influenced by genetic background. J Clin Invest 1999;104:687 – 95.

28. Garami A, Zwartkruis FJ, Nobukuni T, et al. Insulin activation of Rheb, a mediator of mTOR/S6K/4E-BP signaling, is inhibited by TSC1 and 2. Mol Cell 2003;11:1457 – 66.

29. Jaeschke A, Hartkamp J, Saitoh M, et al. Tuberous sclerosis complex tumor suppressor-mediated S6 kinase inhibition by phosphatidylinositide-3-OH kinase is mTOR independent. J Cell Biol 2002;159: 217 – 24.

30. Uhlmann EJ, Apicelli AJ, Baldwin RL, et al. Heterozygosity for the tuberous sclerosis complex (TSC) gene products results in increased astrocyte numbers and decreased p27-Kip1 expression in TSC2+/– cells. Oncogene 2002;21:4050 – 9.

31. Zhang H, Cicchetti G, Onda H, et al. Loss of Tsc1/Tsc2 activates mTOR and disrupts PI3K-Akt signaling through downregulation of PDGFR. J Clin Invest 2003;112:1223 – 33.

32. Kato-Stankiewicz J, Hakimi I, Zhi G, et al. Inhibitors of Ras/Raf-1 interaction identified by two-hybrid screening revert Ras-dependent transformation phenotypes in human cancer cells. Proc Natl Acad Sci U S A 2002;99:14398 – 403.

33. Adjei AA, Davis JN, Erlichman C, Svingen PA, Kaufmann SH. Comparison of potential markers of farnesyltransferase inhibition. Clin Cancer Res 2000;6:2318 – 25.

34. Soucek T, Yeung RS, Hengstschlager M. Inactivation of the cyclin-dependent kinase inhibitor p27 upon loss of the tuberous sclerosis complex gene-2. Proc Natl Acad Sci U S A 1998;95:15653 – 8.

35. Zhang FL, Casey PJ. Protein prenylation: molecular mechanisms and functional consequences. Annu Rev Biochem 1996;65:241 – 69.

36. Kenerson HL, Aicher LD, True LD, Yeung RS. Activated mammalian target of rapamycin pathway in the pathogenesis of tuberous sclerosis complex renal tumors. Cancer Res 2002;62:5645 – 50.

37. Kenerson H, Dundon TA, Yeung RS. Effects of rapamycin in the Eker rat model of tuberous sclerosis complex. Pediatr Res 2004;57:67 – 75.

38. El-Hashemite N, Walker V, Zhang H, Kwiatkowski DJ. Loss of Tsc1 or Tsc2 induces vascular endothelial growth factor production through mammalian target of rapamycin. Cancer Res 2003;63:5173 – 7.

39. Porkka KP, Visakorpi T. Molecular mechanisms of prostate cancer. Eur Urol 2004;45:683 – 91.

40. Zhou BP, Hung MC. Dysregulation of cellular signaling by HER2/neu in breast cancer. Semin Oncol 2003;30:38 – 48.

41. Mitsiades CS, Mitsiades N, Koutsilieris M. The Akt pathway: molecular targets for anti-cancer drug development. Curr Cancer Drug Targets 2004;4:235 – 56.

42. Goncharova E, Goncharov D, Noonan D, Krymskaya VP. TSC2 modulates actin cytoskeleton and focal adhesion through TSC1-binding domain and the Rac1 GTPase. J Cell Biol 2004;167:1171 – 82.

43. Lamb RF, Roy C, Diefenbach TJ, et al. The TSC1 tumour suppressor hamartin regulates cell adhesion through ERM proteins and the GTPase Rho. Nat Cell Biol 2000;2:281 – 7.

44. Astrinidis A, Cash TP, Hunter DS, Walker CL, Chernoff J, Henske EP. Tuberin, the tuberous sclerosis complex 2 tumor suppressor gene product, regulates Rho activation, cell adhesion and migration. Oncogene 2002; 21:8470 – 6.

45. Kim DH, Sabatini DM. Raptor and mTOR: subunits of a nutrient-sensitive complex. Curr Top Microbiol Immunol 2004;279:259 – 70.

46. Im E, von Lintig FC, Chen J, et al. Rheb is in a high activation state and inhibits B-Raf kinase in mammalian cells. Oncogene 2002;21:6356 – 65.

47. Karbowniczek M, Cash T, Cheung M, Robertson GP, Astrinidis A, Henske EP. Regulation of B-Raf kinase activity by tuberin and Rheb is mTOR independent. J Biol Chem 2004;279:29930 – 7.

48. Pritchard CA, Hayes L, Wojnowski L, Zimmer A, Marais RM, Norman JC. B-Raf acts via the ROCKII/LIMK/Cofilin pathway to maintain actin stress fibers in fibroblasts. Mol Cell Biol 2004;24:5937 – 52.

49. Sarbassov dos D, Ali SM, Kim DH, et al. Rictor, a novel binding partner of mTOR, defines a rapamycin-insensitive and raptor-independent pathway that regulates the cytoskeleton. Curr Biol 2004;14: 1296 – 302.

50. Jacinto E, Loewith R, Schmidt A, et al. Mammalian TOR complex 2 controls the actin cytoskeleton and is rapamycin insensitive. Nat Cell Biol 2004;6:1122 – 8.

Molecular Cancer Therapeutics

Farnesyltransferase inhibitors reverse altered growth and distribution of actin filaments in *Tsc*-deficient cells via inhibition of both rapamycin-sensitive and -insensitive pathways

Chia-Ling Gau, Juran Kato-Stankiewicz, Chen Jiang, et al.

Mol Cancer Ther 2005;4:918-926.